



Green synthesis of Zr(IV)aluminophosphate nanoparticles using psyllium husk mucilage for the photodegradation of crystal violet and Fast sulphon black F

Manita Thakur^{1*}, Ajay Sharma¹, Ajay Kumar² and Vandana¹

¹Department of Chemistry, IEC University, Baddi, HP, India

²Department of Chemistry, Maharaja Agrasen University, Baddi, HP, India
manitathakur1989@gmail.com

Available online at: www.isca.in, www.isca.me

Received 19th May 2021, revised 13th October 2021, accepted 9th December 2021

Abstract

Now a days, green synthesis of nanoparticles using plant extracts (seeds, leaves, roots etc.) are in prodigious trend. In this, sol-gel synthesis of psylliumhusk mucilage/Zr(IV) aluminophosphate (PHM@ZAP) nanoparticles has been designed at fixed temperature. PHM@ZAP nanoparticles was characterized through FTIR, SEM, TEM, XRD, UV-Vis and EDS techniques. TEM images showed cluster of nanoparticles with diameter of 50nm approximately which confirm it was nanomaterial. SEM micrographs illustrates that entire morphology was reformed after the mixing of polymeric chains results porous and rough surface with granular particles. PHM@ZAP was explored for the photodegradation of CV and FSB. Effect of various parameters like effect of time, pH effect, effect of dye concentration and photocatalyst dosage has been studied. It was noticed that PHM@ZAP degraded both CV and FSB to large extent as compared to ZAP. 80.07% and 78.01% of FSB and CV has been degraded by PHM@ZAP within 180 minutes.

Keywords: Psyllium husk mucilage, nanoparticles, photocatalysis, crystal violet, fast sulphon black.

Introduction

At present time, comfort of human desires raised to extreme level and to fulfill our needs we disintegrate our natural resources continuously. The activities like industrialization, population increase and squalor of natural resources leads to unbalancing of environment¹⁻³. As we know, water is primary need of all living organisms but less amount of water is serviceable. Pollutants or waste material degraded its quality. Sources of pollutants/toxins can be textile industries, manufacturing plants, household waste and hospital waste etc⁴⁻⁸.

Biomedical waste containing chemicals like dyes, medicine discarded into water sources leads to degrade its quality. These chemical impart harsh effects on all living beings and environment. Dye concentration at high level can cause various health problems like skin allergy, slow mental development in children and increases rate of cancer. Dyes has been used mainly in the production of different products like textiles, paints, printing inks, plastics and paper industries⁹⁻¹¹. Crystal violet and Fast sulphon black F are carcinogenic dyes obtained from textile or industrial waste. They impart severe diseases viz., renal, hepatic, lungs tumor, skin, eye, digestive and respiratory tract irritation etc. Toxic pollutants should be treated before eject into surroundings¹²⁻¹⁶. Diverse approaches has been introduced for the removal of dyes from wastewater like adsorption, electrochemical treatment, photocatalysis, chemical precipitation and oxidation-reduction¹⁷⁻²². Among all of these,

we have used photocatalytic method due to its unique characteristics like easy to handle and highly efficient^{23,24}.

Present research work engrossed the exclusion of poisonous pollutants using biopolymer based hybrid nanomaterials. Recent studies are focused on the synthesis of natural polymer based nanomaterials. Natural polymer like starch, cellulose, pectin, gelatin, psyllium husk etc. are in great demand due to their low toxicity, cheap and non-biodegradability²⁵⁻²⁸. Blending of biopolymers with inorganic material results the formation of hybrid materials with superior properties i.e. both thermal and chemical²⁹⁻³³. Psyllium husk is a soluble dietary fiber, pale to medium buff-colored powder with slight pinkish tinge and weak characteristic odor obtained from husk of psyllium seeds (Plantagoovata plant).

It is gluten free soluble fiber and used as a laxative. It has several health benefits like glucose control, cardiovascular health, weight loss and reduction of gastrointestinal issues. It is a mixture of polysaccharides pentose, hexose and uronic acids. It is inexpensive, non-toxic and easily available³⁴⁻³⁸. Scheme 1 presents Plantagoovata plant, psyllium husk powder and its structure.

This paper introduced fabrication of psylliumhusk mucilage/Zr(IV)aluminophosphate (PHM@ZAP) nanoparticles. It was characterized by SEM, TEM, EDS, FTIR and XRD. PHM@ZAP was explored for the photodegradation of CV and FSB dye.

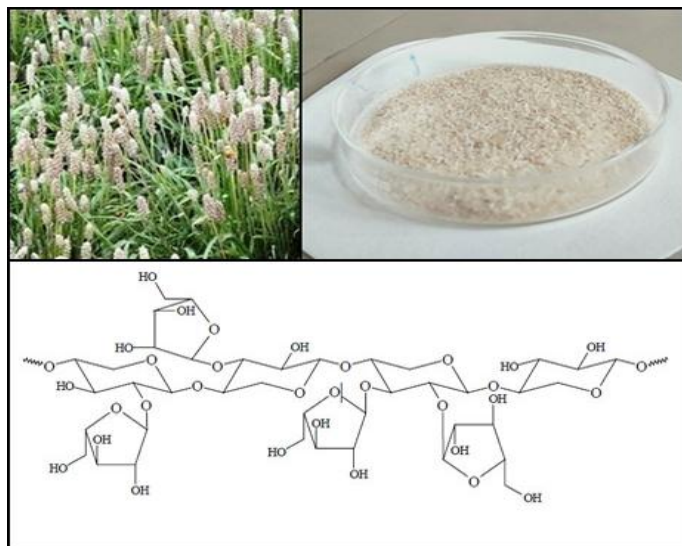


Figure-1: Plantago ovata plant, psyllium husk powder and its structure.

Material and methods

Materials: In present work we used Zirconium oxy chloride, Aluminum phosphate, orthophosphoric acid were purchased from CDH, India. Nitric acid and CV, FSB were procured from Loba Chemie. Psyllium husk was received from local natural products market. All chemicals used in present work were of analytical grade. Stock solutions has been prepared in double distilled water.

Preparation of psyllium husk mucilage (PHM): For this, 10g of psyllium seeds filtered and washed with ethanol (96% w/v) for 15 min with constant stirring 2 to 3 times in order to exclude dust, dirt, stones etc. Seeds were dried at 70°C and disperse clean seeds in 1:100 (w/v) ratio for 1.5 h with constant stirring at 80°C to extract psyllium husk mucilage. Then, mucilage separated through filtration and dried at fixed temperature. Mucilage was stirred for 10 minutes using ethanol in fixed volume ratio (100:75). After that, the above mixture was centrifuged at 1500 rounds per minutes for 5 minutes at room temperature. Supernatant has been used to quantify the non-precipitated carbohydrates and ethanol was isolated from precipitates by using a rotary evaporator³⁹.

Synthesis of psyllium husk mucilage/Zr(IV) aluminophosphate (PHM@ZAP) nanoparticles: Synthesis of PHM@ZAP nanoparticles was designed by following two steps⁴⁰⁻⁴⁴. First step follows, fixed ratio (10:20:10) of 0.1M zirconium oxychloride, 0.1M aluminum phosphate and 0.1M orthophosphoric acid has been put together with continuous stirring at 50-60°C in 500mL beaker. On the other side, gelatinous solution of psyllium husk has been prepared by mixing definite amount of it in distilled water. Onwards, psyllium husk mucilage was transmitted in the above beaker containing ZAP and stirred for 2 hrs at 60°C. After that, above

solution is filtered, precipitates found were washed 2-3 times with demineralized water. By following this route, different samples of varying concentration of psyllium husk mucilage has been synthesized.

Photocatalytic activity: Photocatalytic proficiency of PHM@ZAP nanoparticles was examined against CV and FSB⁴⁵⁻⁴⁸. Different parameters including effect of time, concentration range, pH and amount of photocatalyst was explored onto PHM@ZAP and ZAP. For this, fixed solution of CV and FSB was prepared in double distilled water. Above solutions has been subjected to study the effect of above parameters one to one. Fixed amount of PHM@ZAP and ZAP put into dyes solutions and explored in sun exposure. 5ml of solution withdrawn in fixed intervals of time, centrifuged and record absorbance. In this way, whole process was repeated and percentage degradation was calculated using formula as discussed earlier⁴¹.

Results and discussions

Psyllium husk mucilage/Zr(IV)aluminophosphate nanoparticles was synthesized using sol-gel route. PHM@ZAP nanoparticles has been synthesized by mixing fixed proportion of psyllium husk mucilage in matrix of ZAP at definite temperature. The addition of PHM into ZAP results the formation of new material with tremendous changes in properties, surface and structure. Six samples of different concentration of psyllium husk mucilage has been prepared as shown in Table-1. S-4 was explored for further study due to its superior photocatalytic activity as compared to others.

Table-1: Preparation of different samples of PHM@ZAP nanoparticles.

| S. No | A mol/L | B mol/L | C mol/L | D | pH | Physical appearance | Weight (g) |
|-------|---------|---------|---------|------|-----|---------------------|------------|
| S-1 | 1 | 2 | 1 | - | 0-1 | White | 1.08 |
| S-2 | 1 | 2 | 1 | 0.4% | 0-1 | White | 1.21 |
| S-3 | 1 | 2 | 1 | 0.8% | 0-1 | Light brown | 1.45 |
| S-4 | 1 | 2 | 1 | 1.2% | 0-1 | Light brown | 1.67 |
| S-5 | 1 | 2 | 1 | 1.6% | 0-1 | Brown | 1.91 |
| S-6 | 1 | 2 | 1 | 2.0% | 0-1 | Brown | 2.01 |

Characterization techniques: Figure-2 illustrates FTIR spectra of (a) PHM (b) PHM@ZAP (c) ZAP. Broad peak at 3427cm⁻¹ and 2921cm⁻¹ assigned O-H stretching and O-H, C-H stretching vibrations. 1640cm⁻¹ may be attributed presence of water molecules. Sharp bend at 1048cm⁻¹ and 611cm⁻¹ was due to phosphate group and metal oxide vibrations^{49,50}. It has been

clearly confirmed that formation of PHM@ZAP because after mixing PHM in ZAP merge and reformed new peaks.

Figure-3 shows EDS graph of PHM@ZAP nanoparticles with element weight percentage. The weight percentage of elements were in order of Oxygen (67.13%), Zr (16.63%), P (10.40%), Al (2.71%) and chlorine (0.83%). The given weight percentage of elements confirmed the formation of PHM@ZAP nanoparticles.

Transmission electron micrographs of PHM@ZAP nanoparticles has been given in Figure-4(a-d). Images showed that cluster of nanoparticles with diameter of 50nm approximately. From micrographs, it was noticed that dark black spherical shapes were due to polymeric part and light grey part describes inorganic part. Particles of ZAP were successfully embedded on the polymeric surface which confirmed the formation of PHM@ZAP nanoparticles.

SEM images of psyllium husk mucilage, Zr(IV) aluminophosphate and PHM@ZAP nanoparticles has been shown in Figure-5 (a-b), (c-d) & (e-f). It has been noticed that ZAP has irregular sheets with uneven surface. The entire morphology was reformed after the mixing of polymeric chains into it. Images reflects porous and rough surface with granular particles which was high enough for adsorption of pollutants. Spherical portion in micrographs may represent polymeric part and remaining ZAP.

Figure-6 represents XRD spectra of PHM, ZAP and PHM@ZAP nanoparticles. It has been observed that PH has no sharp peaks which describes its amorphous nature while ZAP has sharp intensity peaks confirms its crystalline nature. But after mixing both, low intensity peaks of PHM@ZAP nanoparticles obtained which confirms its amorphous nature.

Band gap studies: Figure-7(a) shows band gap of PHM@ZAP nanoparticles and determined by using Tauc relation as discussed in literature⁴³. The observed value was 2.26 eV which shows its semiconductor behavior suitable for the photo degradation of FSB and CV.

Photodegradation of crystal violet (CV) and fast sulphon black f (FSB): Figure-7(b) represents mechanism for the photodegradation of FSB and CV by using PHM@ZAP and ZAP. As we can see that when sunlight falls on PHM@ZAP there will be excitation of electrons from VB to CB and generate holes. These released electrons combine with oxygen to form superoxide anion. While, generated holes takes electron from moisture (H₂O) present and became hydroxyl radical. Further, these reactive species i.e. superoxide anion and hydroxyl radical results breaking of organic pollutant into small parts with low toxicity like H₂O and CO₂. PHM@ZAP successfully degraded FSB and CV with higher degradation efficiency. Effect of various parameters has been studied for degradation of FSB and CV as discussed below:

Effect of time on CV and FSB: PHM@ZAP and ZAP were explored to examine effect of time on the degradation efficiency of CV and FSB in different intervals of time from 30 minutes to 5 hours. Figure-8(a) shows that as time increases there was continuous degradation of FSB. It is clearly visible that PHM@ZAP and ZAP degraded 80.07% and 69.12% FSB within 180 minutes. Similarly, Figure-9 (a) illustrates photodegradation of CV using PHM@ZAP and ZAP. It has been found that PHM@ZAP and ZAP degraded 78.01% and 63.15% of CV within 180 minutes. From both Figures we noticed that ZAP has lesser photodegradation potential for FSB and CV as compared to PHM@ZAP nanoparticles. After that, degradation rate for both CV and FSB decreases with increase in time.

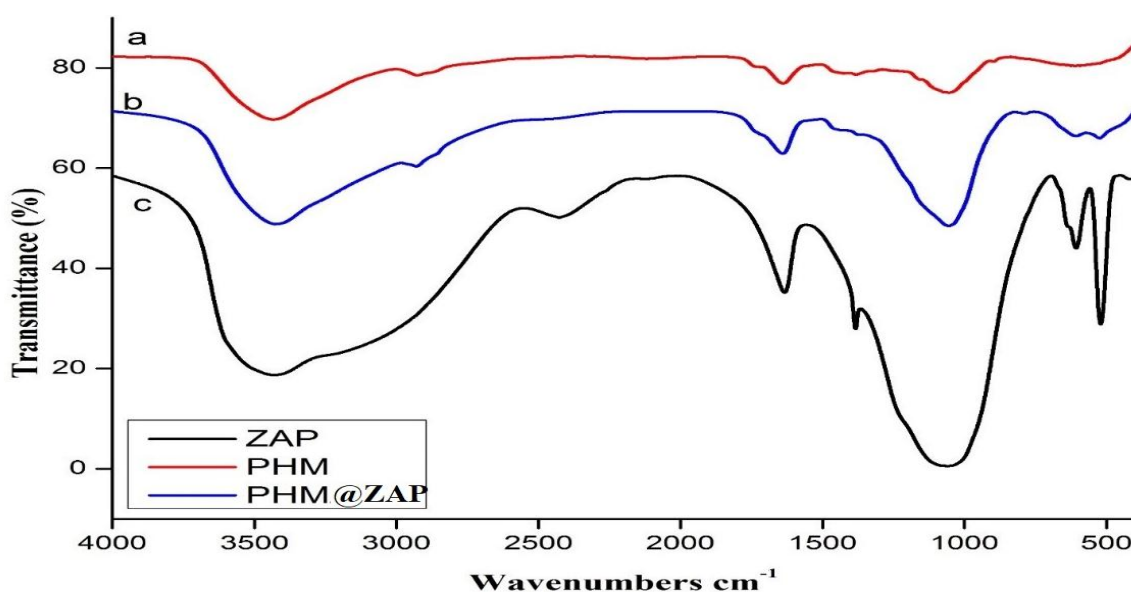


Figure-2: FTIR spectra of (a) PHM (b) PHM@ZAP (c) ZAP.

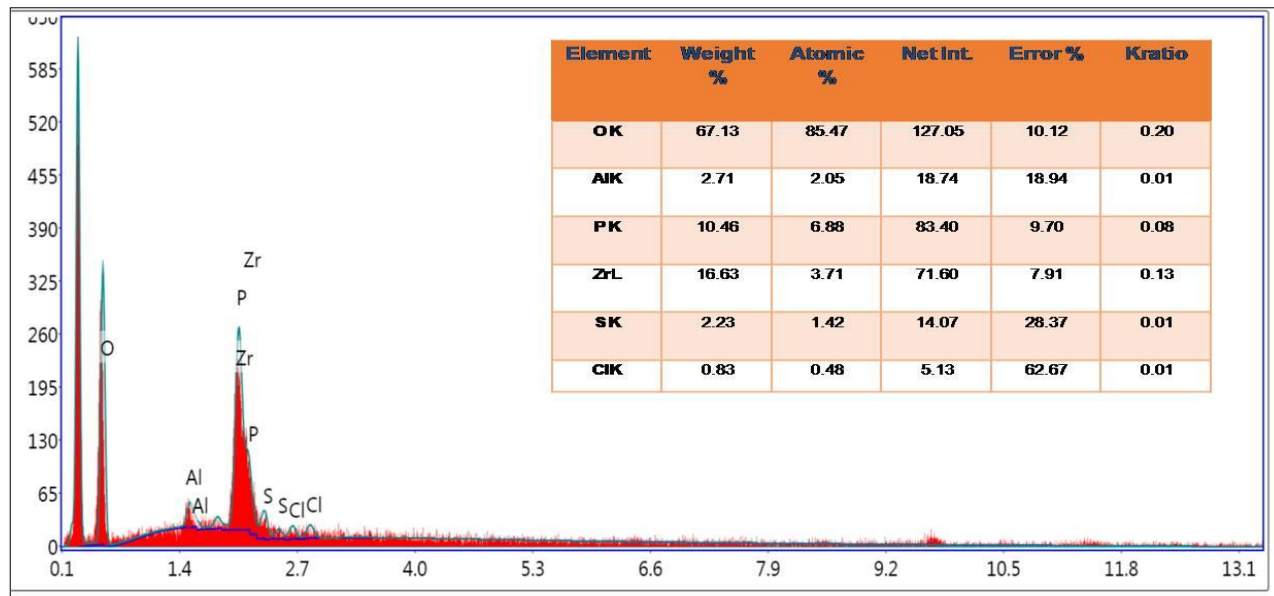


Figure-3: EDS graph of PHM@ZAP nanoparticles.

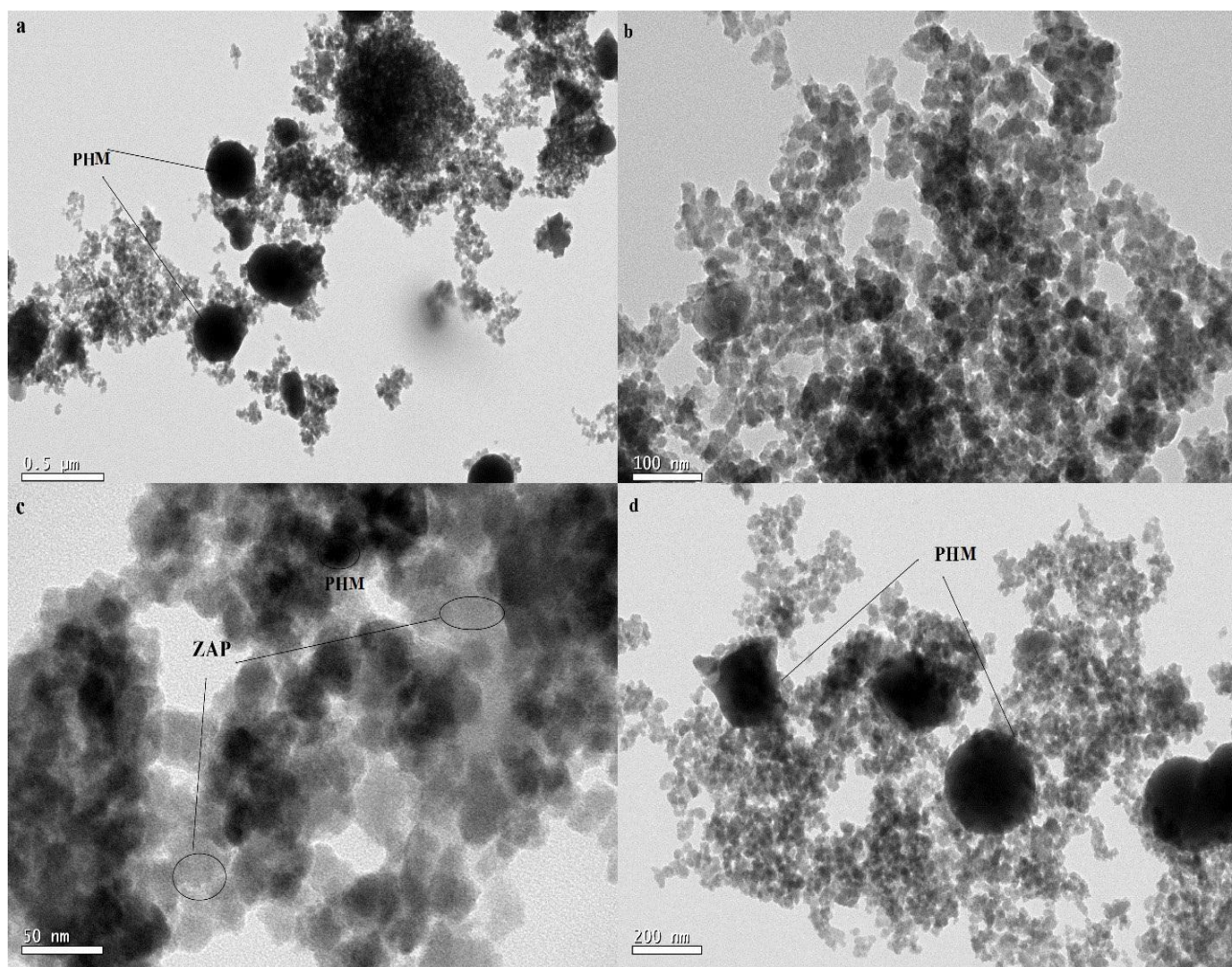


Figure-4: TEM images of PHM@ZAP nanoparticles at different scale.

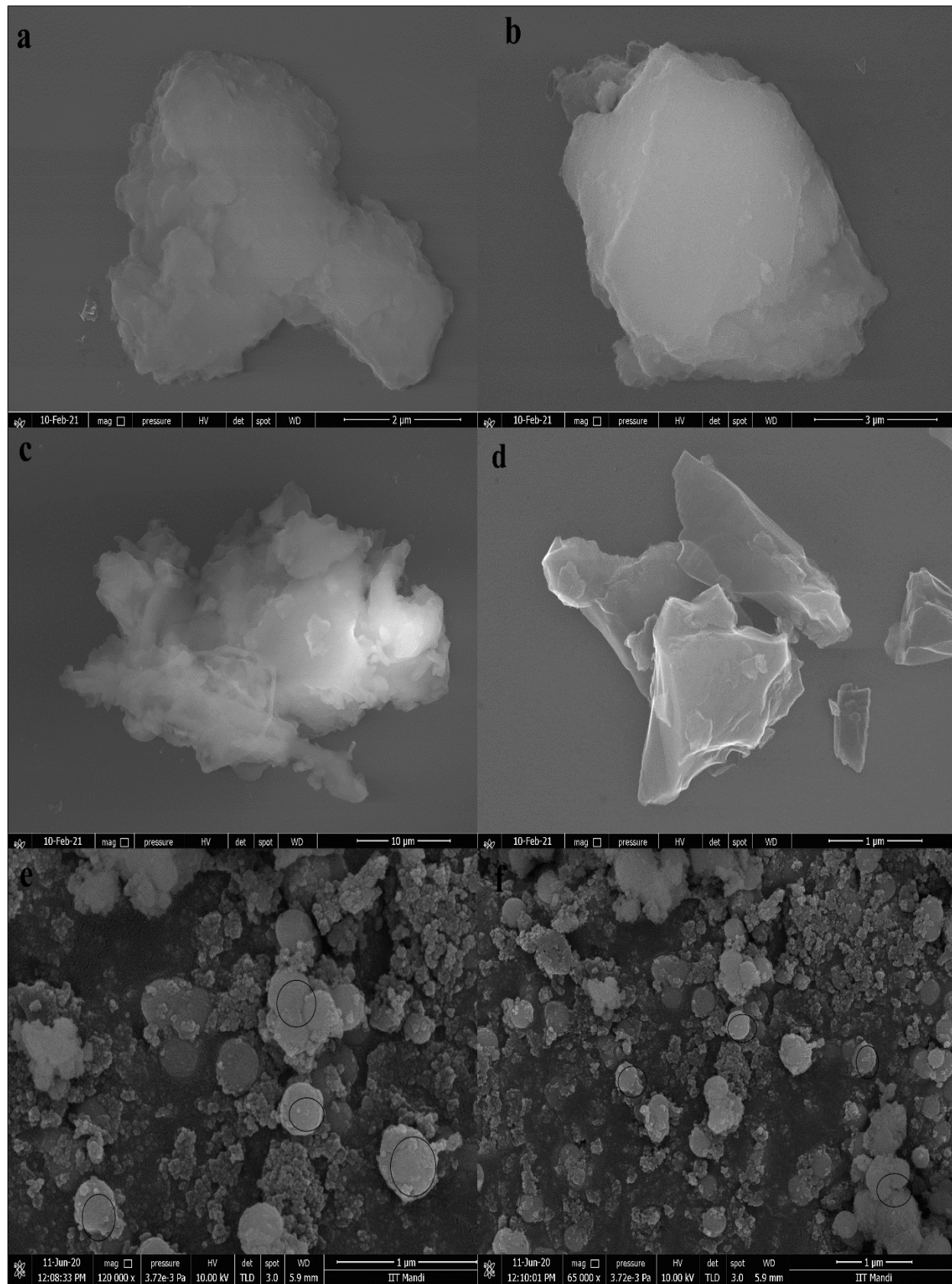


Figure-5: SEM images of (a-b) ZAP (c-d) Psyllium husk mucilage (e-f) PHM@ZAP nanoparticles.

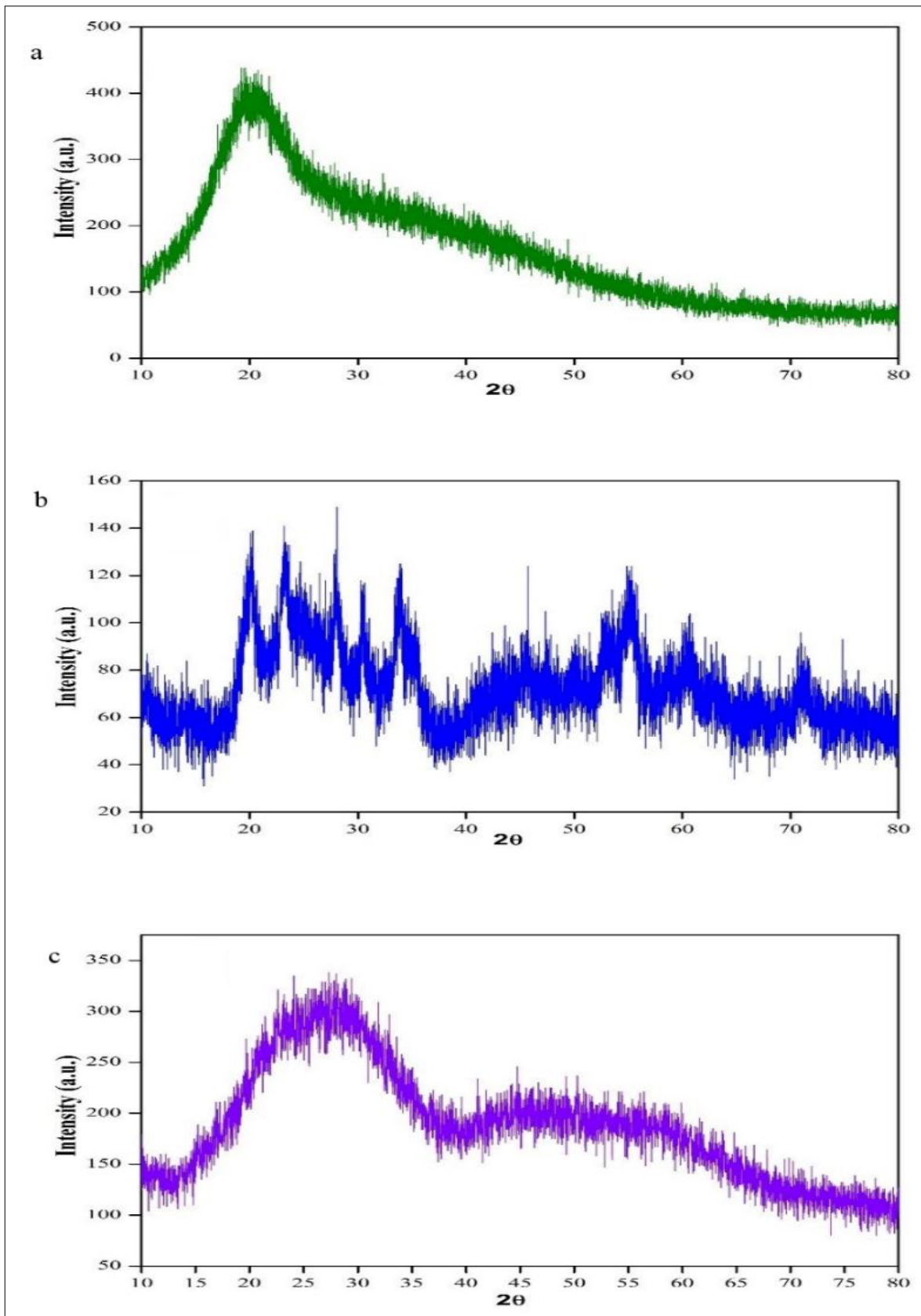


Figure-6: XRD spectra of (a) PHM (b) ZAP (c) PHM@ZAP.

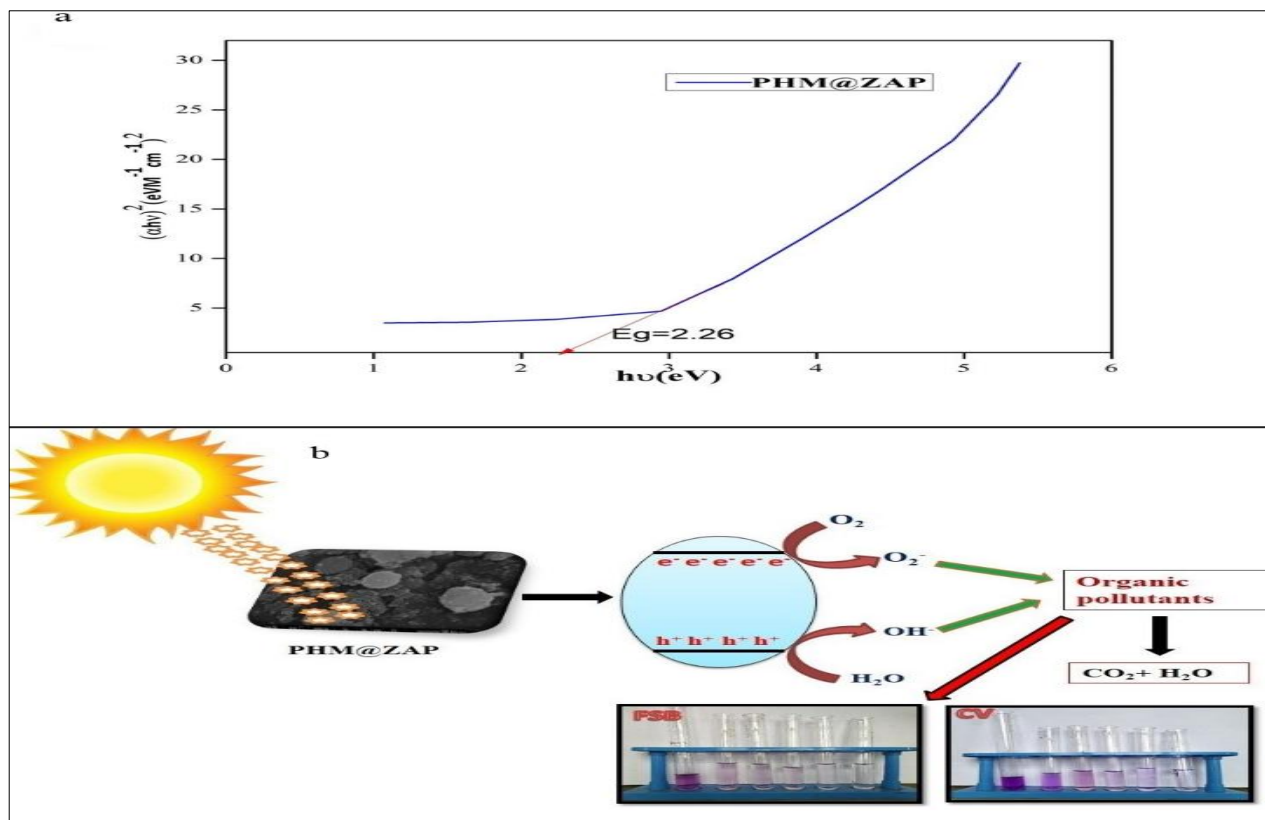


Figure-7: (a) Tauc plot of PHM@ZAP nanoparticles (b) Proposed mechanism for the degradation of CV and FSB.

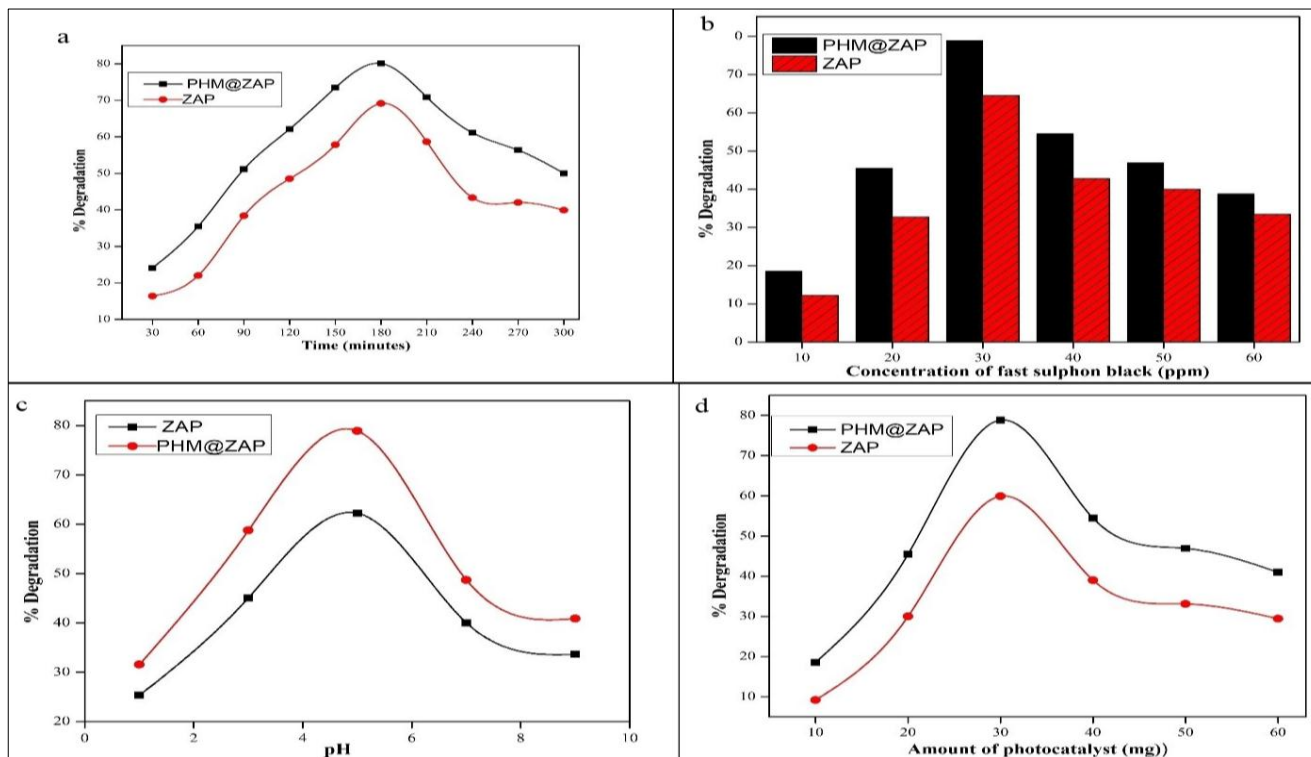


Figure-8: Study of various parameters for the removal of FSB (a) Effect of time on PHM@ZAP & ZAP (b) Effect of FSB concentration (c) pH effect (d) Effect of PHM@ZAP & ZAP dosage.

Effect of concentration on CV and FSB: Figure-8(b) illustrates effect of FSB concentration ranged from 10-60ppm using 30mg of PHM@ZAP and ZAP. It has been noticed that degradation rate increases with increase in concentration upto 10-30ppm for PHM@ZAP and ZAP. Maximum degradation efficiency of PHM@ZAP was 78.84% and 64.56% for ZAP at 30ppm. Further, it get decreased to 38.78% and 33.45% for PHM@ZAP and ZAP at 60 ppm.

Effect of concentration on CV using PHM@ZAP and ZAP is shown in Figure-9(b). Figure shows that maximum degradation of CV was observed at 30ppm. 81.22% and 67.76% degradation was noticed at 30ppm for PHM@ZAP and ZAP and after that it get slightly decreased with increase in concentration.

Effect of pH on photocatalytic activity: Figure-8(c) shows effect of pH on photodegradation efficiency of FSB using PHM@ZAP and ZAP. For this, photocatalytic activity has been performed at different pH range i.e. 1,3,5,7 & 9. From Figure we can see that at pH 5, maximum degradation was found. 78.91% and 62.24% of FSB was degraded by PHM@ZAP and ZAP.

Similarly, effect of pH on CV by using pH/ZAP and ZAP was investigated. Figure-9(c) shows that as pH increases degradation efficiency was also increases upto pH 5. 77.27% and 57.25% of CV was degraded by pH/ZAP and ZAP at pH 5 due to high concentration of H⁺ ions⁴⁴. Further, it drops as pH get increases from 7 to 9.

Effect of amount of photocatalyst i.e. PHM@ZAP and ZAP: Effect of PH/ZAP and ZAP concentration on FSB and CV solutions were studied on different concentration of photocatalysts ranged from 10-60mg. Figure-8 (d) shows the effect of PHM@ZAP and ZAP amount on the photodegradation of FSB. As we can see that from Figure-8 (d), initially

photodegradation rate increases from 18.55% (10mg) upto 78.84% (30mg) for PH/ZAP. Similarly for ZAP it was 9.19% (10mg) to 59.91% (30mg). After that, it was slowly decreases with increasing dose of photocatalyst i.e. PHM@ZAP and ZAP.

Further, Figure-9(d) explored the effect of amount of PHM@ZAP and ZAP on CV degradation. It was clearly apparent that CV degraded continuously from 10-30mg photocatalyst dosage (PHM@ZAP). Maximum degradation efficiency of PHM@ZAP and ZAP was 80.22% and 69.91% at 30mg. After that, it get decreases slowly with increasing amount of photocatalyst.

Figure-10(a & b) represents the degradation of CV and FSB followed by pseudo first-order kinetics. The degradation kinetics of CV and FSB was fitted to pseudo first order kinetics with higher values of rate constant and R² as shown in Table-2. Figure-10(c & d) shows spectra of CV for ZAP and PHM@ZAP with respect to time. It has been observed that intensities of peaks decreases with irradiation time. Similarly, Figure-10(e & f) shows spectra of FSB for ZAP and PHM@ZAP with respect to time.

Table-2: Values of rate constant and R² for photo degradation of FSB and CV using PHM@ZAP & ZAP.

| Sample | Pollutant | K _{app} | R ² |
|---------|-----------|------------------|----------------|
| PHM@ZAP | FSB | 0.016 | 0.998 |
| ZAP | FSB | 0.010 | 0.985 |
| PHM@ZAP | CV | 0.013 | 0.997 |
| ZAP | CV | 0.009 | 0.984 |

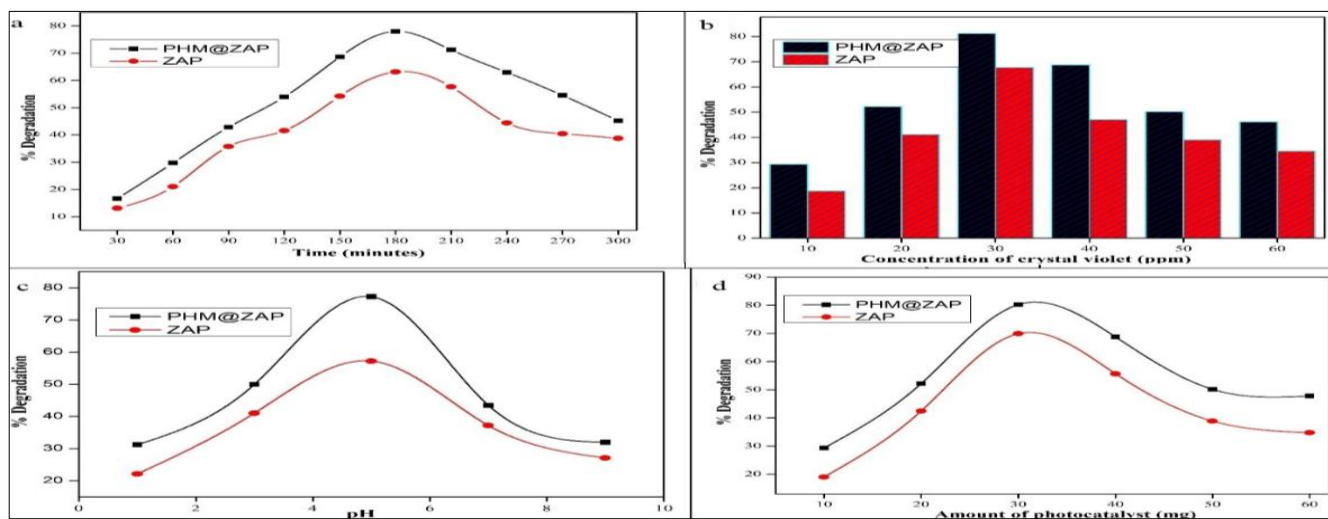


Figure-9: Study of various parameters for the removal of CV (a) Effect of time on PHM@ZAP & ZAP (b) Effect of CV concentration (ppm) (c) pH effect (d) Effect of PHM@ZAP & ZAP dosage.

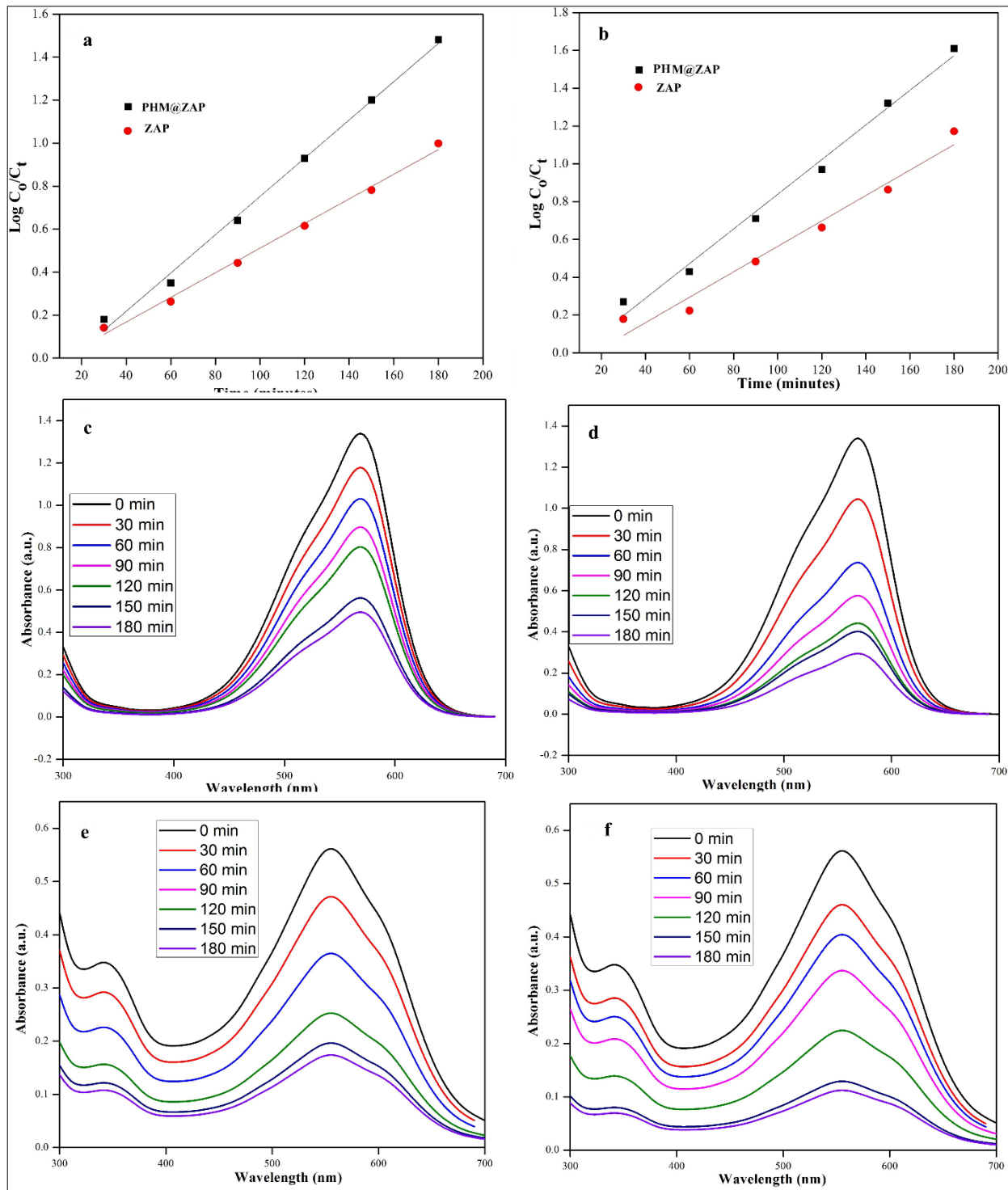


Figure-10: Pseudo first order kinetic model for photodegradation of (a) CV (b) FSB; Absorption spectra of CV for (c) ZAP (d) PHM@ZAP; Absorption spectra of FSB for (e) ZAP (f) PHM@ZAP.

Conclusion

PHM@ZAP nanoparticles were prepared using sol-gel route at fixed pH at 60°C. Nanoparticles were characterized with advanced techniques viz., FTIR, EDS, UV-Vis, SEM, XRD and

TEM. EDS results confirmed the formation of PHM@ZAP with weight percentage of Oxygen (67.13%), Zr (16.63%), P (10.40%), Al (2.71%) and chlorine (0.83%). TEM studies confirmed the formation of particles in nano-range. Band gap of PHM@ZAP nanoparticles was observed to be 2.26 eV which

confirms its semiconductor nature. PHM@ZAP was explored for the photocatalytic removal of CV (78.01%) and FSB (80.07%) with 180 minutes. Effect of time, pH effect, effect of dye concentration and amount of photocatalyst dosage was also studied. Photodegradation of CV and FSB followed by pseudo first-order kinetics with higher values of regression coefficient. PHM@ZAP has potential applications for waste water remediation.

Acknowledgments

Authors would like to extend sincere thanks to IEC University for funding these research facilities.

References

1. Appannagari, R.R. (2017). Environmental pollution causes and consequences: a study. *Int. J. Human. Soc. Sci. Res.* 6, 3(8), 151-61.
2. Schell, L.M. and Denham, M. (2003). Environmental pollution in urban environments and human biology. *Annu. Rev. Anthropol.*, 32, 111-34.
3. Saxena, G. Chandra, R. and Bharagava, R.N. (2016). Environmental pollution, toxicity profile and treatment approaches for tannery wastewater and its chemical pollutants. *Rev environ contam T.*, 240,31-69.
4. Shrivastava, A.K. (2009). A review on copper pollution and its removal from water bodies by pollution control technologies. *Indian j. environ. prot.* 29,552-60.
5. Swami, D. and Buddhi, D. (2006). Removal of contaminants from industrial wastewater through various non-conventional technologies: a review. *Int J Environ Pollut.*, 27,324-46.
6. Thomas, A. (1995). Regulating pollution under asymmetric information: The case of industrial wastewater treatment. *J. Environ. Econ. Manag.*, 28, 357-73.
7. Kadirvelu, K. Karthika, C. Vennilamani, N. and Pattabhi, S. (2005). Activated carbon from industrial solid waste as an adsorbent for the removal of Rhodamine-B from aqueous solution: Kinetic and equilibrium studies. *Chemosphere*, 60, 1009-17.
8. Mirzaei, P. A. and Haghghat, F. (2011). Pollution removal effectiveness of the pedestrian ventilation system. *J. Wind. Eng. Ind. Aerodyn.* 99, 46-58.
9. Kadhom, M. Albayati, N. Alalwan, H. and Al-Furaiji, M. (2020). Removal of dyes by agricultural waste. *Sustain. Chem. Pharm.*, 16, 100259.
10. Yu, Z. Hu, C. Dichiaro, A.B. Jiang, W. and Gu, J. (2020). Cellulose nanofibril/carbon nanomaterial hybrid aerogels for adsorption removal of cationic and anionic organic dyes. *J. Nanomater.*, 10(1), 169.
11. Mao, B. Sidhureddy, B. Thiruppathi, A.R. Wood, P.C. and Chen, A. (2020). Efficient dye removal and separation based on graphene oxide nanomaterials. *New J Chem.*, 44(11), 4519-28.
12. Rao, S.K. Ranyal, R.K. Bhatia, S.S. and Sharma, V.R. (2004). Biomedical waste management: an infrastructural survey of hospitals. *Med J Armed Forces India*, 60, 379-82.
13. Patil, P.M. and Bohara, R.A. (2020). Nanoparticles impact in biomedical waste management. *Waste Manag. Res.*, 38, 1189-203.
14. Gautam, V. Thapar, R. and Sharma, M. (2010). Biomedical waste management: Incineration vs. environmental safety. *Indian J. Med. Microbiol.*, 28, 191.
15. Van de Velde, K. and Kiekens, P. (2002). Biopolymers: overview of several properties and consequences on their applications. *Polym. Test.*, 21, 433-42.
16. Guleria, A. Sharma, R. and Shandilya, P. (2021). Photocatalytic and Adsorptional Removal of Heavy Metals from Contaminated Water using Nanohybrids. *Photocatalysis: Advanced Materials and Reaction Engineering*, 100, 113-60.
17. Shandilya, P. Sambyal, S. Sharma, R. Kumar, A. and Vo, D.V. (2021). Recent Advancement on Ferrite Based Heterojunction for Photocatalytic Degradation of Organic Pollutants: A Review. *Ferrite: Nanostructures with Tunable Properties and Diverse Applications*, 112, 121-61.
18. Shandilya, P. Guleria, A. and Fang, B. (2021). A magnetically recyclable dual step-scheme Bi₂WO₆/Fe₂O₃/WO₃ heterojunction for photodegradation of bisphenol-A from aqueous solution. *J. Environ. Chem. Eng.*, 10, 106461.
19. Guleria, A. Sharma, R. Singh, A. Upadhyay, N.K. and Shandilya, P. (2021). Direct dual-Z-scheme PANI/Ag₂O/Cu₂O heterojunction with broad absorption range for photocatalytic degradation of methylene blue. *J. Water Process. Eng.*, 43, 102305.
20. Shandilya, P. Mandyal, P. Kumar, V. and Sillanpaa, M. (2021). Properties, synthesis, and recent advancement in photocatalytic applications of graphdiyne: a review. *Sep. Purif. Technol.*, 19825.
21. Shandilya, P. Sharma, R. Arya, R.K. Kumar, A. Vo, D.V. and Sharma, G. (2021). Recent progress and challenges in photocatalytic water splitting using layered double hydroxides (LDH) based nanocomposites. *Int. J. Hydrog. Energy*.
22. Sharma, R. Arizaga, G.G. Saini, A.K. and Shandilya, P. (2021). Layered double hydroxide as multifunctional materials for environmental remediation: From chemical pollutants to microorganisms. *Sustain. Mater. Technol.* e00319.
23. Morshed, M.N. Al Azad, S. Deb, H. Shaun, B.B. and Shen, X.L. (2020). Titania-loaded cellulose-based functional

- hybrid nanomaterial for photocatalytic degradation of toxic aromatic dye in water. *J. Water Process. Eng.*, 33, 101062.
24. Shandilya, P. Raizada, P. Sudhaik, A. Saini, A. Saini, R. and Singh, P. (2021). Metal and Carbon Quantum Dot Photocatalysts for Water Purification. *In Water Pollution and Remediation: Photocatalysis*, 81-118.
 25. Kurita, K. (2006). Chitin and chitosan: functional biopolymers from marine crustaceans. *Mar. Biotechnol.*, 8, 203-26.
 26. Rao, M. Bharathi, G. P. and Akila, R.M. (2014). A comprehensive review on biopolymers. *Sci. Revs. Chem. Commun.*, 4, 61-8.
 27. Giesa, T. and Buehler, M.J. (2013). Nanoconfinement and the Strength of Biopolymers. *Annu. Rev. Biophys.*, 42, 651-73.
 28. George, A. Sanjay, M.R. Srisuk, Parameswaranpillai, R. and Siengchin, J. S. (2020). A comprehensive review on chemical properties and applications of biopolymers and their composites. *Int. J. Biol. Macromol.*, 154, 329-38.
 29. Lapointe, M. and Barbeau, B. (2020). Understanding the roles and characterizing the intrinsic properties of synthetic vs. natural polymers to improve clarification through interparticle Bridging: A review. *Sep Purif Technol.*, 231, 115893.
 30. Donato, R.K. and Mija, A. (2020). Keratin associations with synthetic, biosynthetic and natural polymers: An extensive review. *Polymers*, 12, 32.
 31. Sell, S.A. Wolfe, P.S. Garg, K. McCool, J.M. Rodriguez, I.A. and Bowlin, G.L. (2010). The use of natural polymers in tissue engineering: a focus on electrospun extracellular matrix analogues. *Polymers.*, 2, 522-53.
 32. Martina, M. and Hutmacher, D.W. (2007). Biodegradable polymers applied in tissue engineering research: a review. *Polym. Int.*, 56, 145-57.
 33. Garg, A. Garg, S. Kumar, M. Kumar, S. Shukla, A.K. and Kaushik, S.P. (2018). Applications of natural polymers in mucoadhesive drug delivery: An overview. *Adv. Pharm. J.*, 38-42.
 34. Mehmood, M. H. Aziz, N. Ghayur, M.N. and Gilani, A.H. (2011). Pharmacological basis for the medicinal use of psyllium husk (Ispaghula) in constipation and diarrhea. *Dig. Dis. Sci.*, 56, 1460-71.
 35. Giacosa, A. and Rondanelli, M. (2010). The right fiber for the right disease: an update on the psyllium seed husk and the metabolic syndrome. *J. Clin. Gastroenterol.*, 44, S58-60.
 36. Qaisrani, T.B. Butt, M.S. Hussain, S. and Ibrahim, M. (2014). Characterization and utilization of psyllium husk for the preparation of dietetic cookies. *Int. J. Mod. Agric.*, 3, 81-91.
 37. Sukhija, S. Singh, S. and Riar, C.S. (2016). Analyzing the effect of whey protein concentrate and psyllium husk on various characteristics of biodegradable film from lotus (*Nelumbonucifera*) rhizome starch. *Food Hydrocoll.*, 60, 128-37.
 38. Gharibzahedi, S.M. Razavi, S.H. and Mousavi, S.M. (2013). Psyllium husk gum: An attractive carbohydrate biopolymer for the production of stable canthaxanthin emulsions. *Carbohydr. Polym.*, 92, 2002-11.
 39. Ladjevardi, Z.S. Gharibzahedi, S.M. and Mousavi, M. (2015). Development of a stable low-fat yogurt gel using functionality of psyllium (*Plantago ovata* Forsk) husk gum. *Carbohydr. Polym.*, 125, 272-80.
 40. Pathania D., Thakur M. and Mishra A.K. (2017). Alginate-Zr (IV) phosphate nanocomposite ion exchanger: Binary separation of heavy metals, photocatalysis and antimicrobial activity. *J. Alloys Compd.*, 701, 153-62.
 41. Thakur, M. and Pathania, D. (2019). Sol-gel synthesis of gelatin-zirconium (IV) tungstophosphate nano composite ion exchanger and application for the estimation of Cd (II) ions. *J Solgel Sci Technol.*, 89, 700-12.
 42. Pathania, D. Thakur, M. Puri, V. and Jasrotia, S. (2018). Fabrication of electrically conductive membrane electrode of gelatin-tin (IV) phosphate nanocomposite for the detection of cobalt (II) ions. *Adv Powder Technol.*, 29, 915-24.
 43. Pathania, D. Agarwal, S. Gupta, V.K. Thakur, M. and Alharbi, N.S. (2018). Zirconium (IV) phosphate/poly (gelatin-cl-alginate) nanocomposite as ion exchanger and Al³⁺ potentiometric sensor. *Int. J. Electrochem. Sci.* 13, 994-1012.
 44. Abou Hammad, A.B. Elnahrawy, A.M. and Youssef, A.M. (2019). Sol gel synthesis of hybrid chitosan/calcium aluminosilicate nano composite membranes and its application as support for CO₂ sensor. *Int. J. Biol. Macromol.*, 125, 503-9.
 45. Pathania, D. Thakur, M. Sharma, G. and Mishra, A.K. (2018). Tin (IV) phosphate/poly (gelatin-cl-alginate) nanocomposite: Photocatalysis and fabrication of potentiometric sensor for Pb (II). *Mater. Today Commun.*, 14, 282-93.
 46. Gupta, V. Sharma, G. Kumar, A. and Stadler, F.J. (2019). Preparation and characterization of Gum Acacia/Ce (IV) MoPO₄ nanocomposite ion exchanger for photocatalytic degradation of methyl violet dye. *J Inorg Organomet Polym Mater.*, 29, 1171-83.
 47. Jeyasubramanian, K. Hikku, G.S. and Sharma, R.K. (2015). Photo-catalytic degradation of methyl violet dye using zinc oxide nano particles prepared by a novel precipitation method and its anti-bacterial activities. *Water Process. Eng.*, 8, 35-44.

48. Liu, G. and Zhao, J. (2000). Photocatalytic degradation of dye sulforhodamine B: a comparative study of photocatalysis with photosensitization. *New J. Chem.*, 24, 411-7.
49. Ren, X. Xu, D. Yin, Y. Zou, X. Wang, Y. Shang, X. and Wang, X (2021). High Catalytic Performance and Sustainability of Zr Modified Aluminophosphate for Vapor-Phase Selective O-Methylation of Catechol with Methanol. *Catalysts.*, 11, 740.
50. Sreenivasulu, P. Viswanadham, N. Sharma, T. and Sreedhar, B. (2014). Synthesis of orderly nanoporous aluminophosphate and zirconium phosphate materials and their catalytic applications. *Chem Comm.*, 50, 6232-5.